US Open Electrical & Electronics Engineering Journal
Vol. 1, No. 1, July 2015, pp. 1-16
Available online at http://arepub.com/Journals.php

Research article

A Tutorial Application of the Method of Moments using with an Expansion Function the Haar Wavelet to Solve Many Electrostatic Problem

Aldo Artur Belardi and Antonio Honorato Piciniinin Neto

E-mail: belardi@fei.edu.br

Abstract

This paper presents the mathematical basis, and some results, concerning the application of the Haar Wavelets as the expansion function in the Method of Moments. As an example, the surface charge density on a finite, thin plane plate, and the Eddy current problem, in which the main computational performance aspects are evaluated. Some computational optimization techniques are used, and their main aspects are stressed in the paper.

Key Words: Moments, Wavelets, Haar

I. INTRODUCTION

Regarding the formulation, in order to illustrate the proposed methodology, the main theoretical aspects of the Method of Moments and of the Haar wavelets, are here presented. For simplification, the one and two dimension applications are taken into consideration.

a. Method of Moments

Although the Method of Moments is a known numerical one, and the complete description and details of this method have already been presented in many papers, in order to guide the reader through the overall method explanation, a brief summary is here shown. In a simplified way, it can be mentioned that the basis of the Method of Moments is the application of approximation functions, like the following one [1].

$$f(x) = \sum_n \alpha_n L g_n \qquad (1)$$

In the aforementioned expression, α_n is the unknown coefficients, g_n is the expansion function, the pulse or the Haar wavelets, and "**L**" a mathematical operator. When the inner product, using a weighed function W_m, is carried out.

$$\sum_n \alpha_n < L g_n, W_m > = < f, W_m > \quad \text{para} \quad m = 1, 2 ..... N \qquad (2)$$

The previous expression can be represented in a matrix form by [A][α]=[B], where [α] is the unknown approximated solution coefficients column vector, and the matrixes [A] and [B] are given by:

$$\left[A\right]=\begin{bmatrix} < \boldsymbol{L}g_1, W_1 > & .... < \boldsymbol{L}g_n, W_1 > \\ < \boldsymbol{L}g_1, W_2 > & \ldots < \boldsymbol{L}g_n, W_2 > \\ < \boldsymbol{L}g_1, W_n > & .... < \boldsymbol{L}g_n, W_n > \end{bmatrix};\left[B\right]=\begin{bmatrix} < f, W_1 > \\ < f, W_2 > \\ < f, W_n > \end{bmatrix} \quad (3)$$

As a first application, the potential distribution on a finite and straight wire that can be calculated using the next equation is taken into consideration [2]:

$$V\left(x, y=0, z=0\right)=\frac{1}{4\pi\varepsilon}\int\frac{\rho(r')}{R\left(x,x'\right)}dl' \quad (4)$$

Thus making use of the method of moments, knowing the approximated solution function f(x), the expansion function g(x) and the weighting function W(x), the potential on a finite straight wire can be estimated by the inner product of these functions:

$$V(x)=\left\langle g, W, f\right\rangle\frac{1}{R}=\int_{-a}^{a}\frac{g\left(x\right)W\left(x\right)f\left(x\right)}{R\left(x\right)}dx \quad (5)$$

Consequently, the surface density can be approximated by the N term expansion. If the wire is divided into uniform segments $\Delta=L/N$, after applying the weight delta function of Dirac $W_m = \delta(x_m – x') = 1$, the inner product will become:

$$V(x)=\left\langle W_m\delta, f, \boldsymbol{L}g x\right\rangle = \quad x\left(\quad - \quad _m\right)$$

$$x\alpha\frac{1}{4\pi\varepsilon}\sum_{n=1}^{N}\int_{0}^{L_n}\frac{g_n(x')}{\sqrt{(x_m-x')^2+a^2}}dx' \quad (6)$$

Assuming the charges placed in the center of each subdivision in relation to the axis, substituting the values of x by the distance of the charge position to the point $P(x_m)$, we will have an integral that is only function of the x'. For a fixed potential V, the equation can be represented, using matrix notation, by $[V_m] = [Z_{mn}]\ [\alpha_n]$, in which Z_{mn} is defined by [3]:

$$Z_{mn}=\int_{0}^{L}\frac{g_n(x')}{\sqrt{(x_m-x')^2+a^2}}dx' \quad (7)$$

The same approach can be used, if a two-dimensional application is considered. If a square plane plate is considered as an example, we should remember that the potential in a finite and very thin plane plate can be evaluated by [4]:

$$V(x,y,z=0)=\frac{1}{4\pi\varepsilon}\int_{-a}^{a}\rho(x',y')dx'\int_{-b}^{b}\frac{dy'}{[(x-x')^2+(y-y')^2]^{1/2}} \quad (8)$$

Thus, after applying the method of the moments, knowing the function of the approximated solution f(x,y), the expansion function g(x,y) and the weighed function W(x,y), the potential in a square plane plate, will be estimated by the inner product of these functions [5]:

$$V(x,y)=\left\langle g, W, f\right\rangle\frac{1}{R}=\int_{-a}^{a}\frac{g(x,y)W(x,y)f(x,y)}{R\left(x,y\right)}dx \quad (9)$$

where,

$$R(x,y) = \sqrt{(x - x')^2 + (y - y')^2} \qquad (10)$$

Dividing the plate in equal segments and applying the weighed function as being the delta function of Dirac, we had that $W_m = \delta(x - x_m)\delta(y - y_m)$, being the inner product in the point given by:

$$V(x,y,z=0) = \langle W_m, fg \rangle = \delta(y - y_m)(x - x_m) \times$$

$$\times \frac{1}{4\pi\varepsilon} \int_{-a}^{a} dx' \int_{-b}^{b} dy' \frac{\sum_{n=1}^{N} \alpha_n g_n(x',y')}{[(x_m - x')^2 + (y_m - y')^2]^{1/2}} \qquad (11)$$

Assuming the charges placed in the center of each sub division in relation to each axes, substituting the values of x and y by the distance of the charge position to the point P(x_m , y_m), we will have an integral that is only function of x' e y'. For a fixed potential V, the equation can be represented, using the matrix notation, by $[V_m]=[Z_{mn}][\alpha_n]$, in which Z_{mn} is defined by:

$$Z_{mn} = \int_{-a}^{a} dx' \int_{-b}^{b} \frac{g_n(x',y')}{4\pi\varepsilon\sqrt{(x_m - x')^2 + (y_m - y')^2}} dy' \qquad (12)$$

b. The Wavelets

The analysis through the wavelets has been a good alternative in replacement of the classical analyses that utilize the Fourier series, chiefly when treating acoustic signals, interpreting seismic signals and in the solution of numerical methods applied to electromagnetism and electrostatics [6][7][8]. In general the wavelets can be defined by:

$$\psi_{a,b}(x) = |a|^{-1/2} \psi\left(\frac{x - b}{a}\right) \quad a,b \in R, a \neq 0 \qquad (13)$$

Some kinds of wavelets are mentioned in the literature, making it possible for new family models to be built from them, which adapt more appropriately to each case. Fig. 1 represents the Morlet or Modulated Gaussian wavelet, which is expressed by:

$$\psi(x) = e^{i\omega_0 x} e^{-x^2/2} \qquad (14)$$

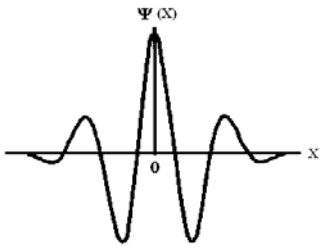

Fig. 1 - Morlet

The Fig. 2 represents the Mexican hat wavelet, which is expressed by:

$$\psi(x) = (1 - x^2)e^{-x^2/2} \qquad (15)$$

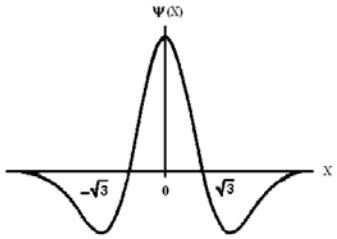

Fig. 2 - Mexican hat

The Fig. 3 represents the Shannon wavelet, which is expressed by:

$$\psi(x) = \frac{\sin(\frac{\pi x}{2})}{\frac{\pi x}{2}} \cos(\frac{3\pi x}{2})$$

$$\varphi(x) = \begin{cases} \frac{\sin(\pi x)}{\pi x}, & x \neq 0 \\ 1, & x = 0 \end{cases} \qquad (16)$$

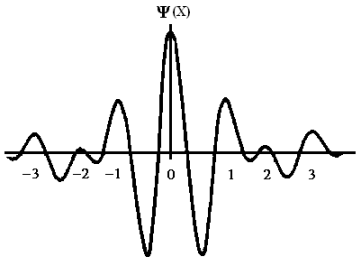

Fig. 3 - The Shannon wavelet

c. The Haar Wavelets

It was previously mentioned that many functions can be used as the expansion function: Among them, the pulse function, the truncate cosine function and the wavelets can be mentioned. Thus, after applying the method of the moments, and considering the Haar wavelets, a function f(x,y) can be approximated by:

$$f(x,y) = \sum_{k=-\infty}^{\infty} c_k \phi(x,y) + \sum_{j=-\infty}^{\infty} \sum_{k=-\infty}^{\infty} d_{j,k} f_P(x,y) \quad _{j,k}(\quad) \qquad (17)$$

In this equation “j”, and “k” are the resolution and the translation levels, respectively.
Moreover, once the Haar wavelets, and the so-called mother function and scale function father are applied, the formulation, for two-dimensional applications, will result in a product combination, given by [9][10]:

$$\phi^{(H)}(x) = \begin{cases} 1 & 0 \leq x < 0.5, \text{ and} \\ 0 & \text{for other intervals} \end{cases} \qquad (18)$$

$$\psi_{j,k}^{(H)}(x)=\left[\ \phi(x)\ \psi(x)\psi(2x)\psi(2x-1)\ldots\psi\left(2^{j}x-k\right)\right]$$

$$\psi_{j,k}^{(H)}(y)=\left[\ \phi(y)\ \psi(y)\psi(2y)\psi(2y-1)\ldots\psi\left(2^{j}y-k\right)\right] \quad (19)$$

$$\left\{\psi_{j,k}^{(H)}(x),(y)\right\}=\phi(x)\phi(y),\phi(x)\psi(y),\ldots,\psi(2x-1)\psi(2y-1)$$

II. FORMULATION

a. Finite Straight

Thus, making use of the method of moments, and the wavelets the Haar the potential on a finite straight wire can be estimated by the inner product of these functions. As an illustration, the Fig. 4 represents the Haar function regarding one dimensions and two level of resolution [11].

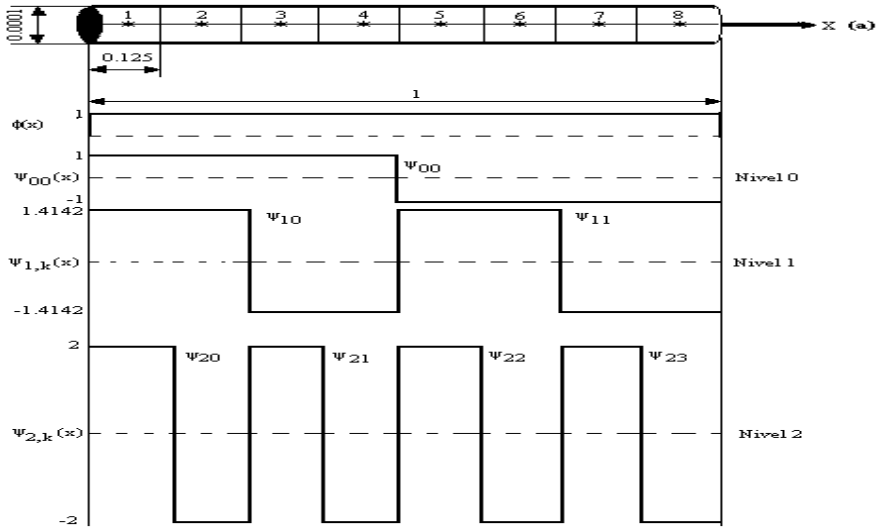

Fig. 4 - The Haar wavelet in a finite straight

The mathematical solution is:

$$V(r)=\frac{1}{4\pi\varepsilon}\left[\int_{0}^{L}\frac{c_0\phi(x)}{R(x,x')}dx+\int_{0}^{L}\frac{\sum_{n=1}^{N}c\psi_{j,k}\ \psi_{j,k}^{(H)}(\ )}{R(x,x')}dx\right] \quad (20)$$

$$V(r)=\frac{1}{4\pi\varepsilon}\int_{0}^{L}\frac{\phi(x)}{\sqrt{(x-x')^2+a^2}}dx+\left[\sum_{j=-\infty}^{\infty}\sum_{k=-\infty}^{\infty}c_{j,k}\int_{0}^{L}\frac{\psi_{j,k}^{(H)}(x')}{\sqrt{(x-x')^2+a^2}}dx\right] \quad (21)$$

b. The thin plane plate

The same approach can be used, if a two-dimensional application is considered. It was previously mentioned that many functions can be used as the expansion function. Among them, the pulse function, the truncate cosine function and the wavelets, the general aspects of the wavelets are shown. As an illustration, the Fig. 5 represents the Haar function regarding two dimensions and one level of resolution, for a point P(x_m, y_m). On the other hand, if the potential in a finite and very thin plane plate is taken into account as an application, it can be evaluated by[12]:

At each point we have:

$$V(x,y) = \int_{-a}^{a}\int_{-b}^{b} \frac{\phi(x,y)}{\sqrt{(x_m-x')^2+(y_m-y')^2}}dxdy + \sum_{j=-\infty}^{\infty}\sum_{k=-\infty}^{\infty} a_{j,k}b_{j,k}\int_{-a}^{a}\int_{-b}^{b}\frac{\psi_{j,k}^{(H)}(x,y)}{\sqrt{(x_m-x')^2+(y_m-y')^2}}dxdy \quad (22)$$

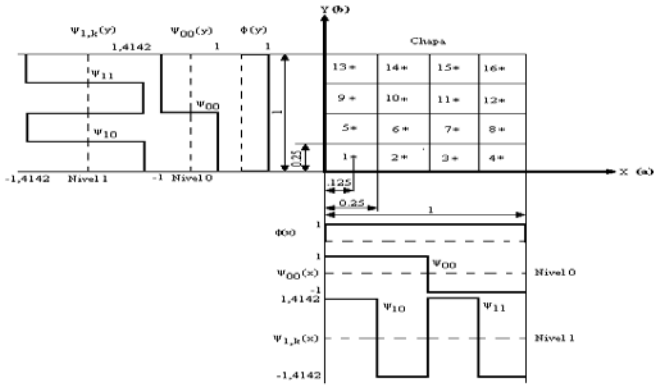

Fig.5 - Representation of the Haar function for two-dimensions and one level of resolution.

At each point we have:

$$\left\{c_k\psi_{j,k}^{(H)}\, d_{j,k}\psi_{j,k}^{(H)}\right\} = a_0b_0\phi(x)\phi(y)+a_0b_{00}\phi(x)\psi_{00}(y)+a_0b_{10}\phi(x)\psi_{10}(2y) + a_0b_{11}\phi(x)\psi_{11}(2y-1)+a_{00}b_0\psi_{00}(x)\phi(y)+\ldots+a_{11}b_{11}\psi_{11}(2x-1)\psi_{11}(2y-1) \quad (23)$$

c. The Eddy Current problem

Let us consider the conducting wire to be composed of filaments, having their length is represented by c and current density by J(r'), according to Fig. 6.

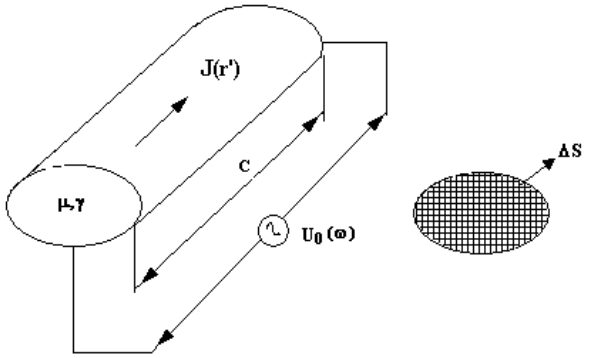

Fig. 6 - Current in the conductor

The two-dimensional fields can be obtained by using two or more current distributions J_1, J_2... on surface S, which is the interface between the conductor and the air.
By integrating it is possible to simplify the equations the most, so that there will not be complex integrals or approximations, as follows [13][14]:

$$A(r) = \frac{\mu}{2\pi}\int_s J(r')\ln\frac{1}{|r-r'|}ds' \qquad (24)$$

In which r and r´ are respectively the origin and source points. The current density can be expressed by:

$$J(r) = J_e(\sigma+j\omega\varepsilon)A_s \mp -j\omega\gamma U(/c)_0 \qquad (25)$$

In which $\mathbf{U_0}$ is the applied voltage, **c** and **s** are the length and the sectional area of the conductor. Considering Fredholm integral, a second order equation is obtained:

$$J(r) = \frac{j\omega\mu\gamma}{2\pi}\int_s J(r')\ln|r-r'|ds' + J_s \qquad (26)$$

In which the math operator in the previous equation is given by:

$$\boldsymbol{L} = 1 - \frac{j\omega\mu\gamma}{2\pi}\int_s \ln|r-r'|ds' \qquad (27)$$

By dividing the domain into N elements, the current density can be approximated by:

$$J(r) \approx \sum_1^n J_1 \qquad (28)$$

By choosing the pulse as the expansion and weighting functions, the coefficients of matrix A can be determined by the following expression [15][16]:

$$a_{mn} = \langle \boldsymbol{L}_n = W_m \rangle \int_s \int_s (\quad) \frac{j\omega\mu\gamma}{2\pi} \int_s \int_s (\quad) \ln\left[(x_m - x_n)^2 + (y_m - y_n)^2\right]^{1/2} P_n(x,y)\,ds\,ds' \qquad (29)$$

or

$$a_{nm} = -\frac{j\omega\mu\gamma}{2\pi}\Delta S_m * \\ *\ln\left[\left(x_m - x_n\right)^2 + \left(y_m - y_n\right)^2\right]^{1/2} \quad (30)$$

$$b_{mn} = \left\langle J_s, W_m \right\rangle = J_s$$

Let us consider the sides of the elements resulting of the divisions performed in the superficial part of the conductor are square and defined as h. By eliminating the other ΔS_m terms in the equations a_{mn} and b_m, considering the relative positions of the different charges that will form the elements of matrix A, and the relations d/h> 2 and d/h=1, the following will be obtained:

$$a_{mn} = 1 - \frac{j\omega\mu\gamma}{4\pi} h^2 \ln\left[\left(x_m - x_n\right)^2 + \left(y_m - y_n\right)^2\right] \quad (31)$$

$$a_{mn} = 1 - 1,0065\frac{j\omega\mu\gamma}{4\pi} h^2 * \\ *\ln\left[\left(x_m - x_n\right)^2 + \left(y_m - y_n\right)^2\right] \quad (32)$$

if m=n

$$a_{mn} = 1 - \frac{j\omega\mu\gamma}{2\pi} h^2 \ln\left(0,44705h\right) \quad (33)$$

By solving matrix $A\{J\}=\{J_s\}$ the current matrix will be obtained.

III. APPLICATION

a. Finite wire

Applying the aforementioned formulation, we got some results related to two applications: the first one related to a finite and straight wire, and another one regarding a thin plane plate. It is assumed in the two applications a constant potential distribution equal to1V, conform Fig. 7.
Table I presents the results regarding the charge surface density on a 1.0m straight wire, when it is divided in to 16 equal segments, as a function of the resolution (j) and the translation (k) levels. Those results can be considered as the ones suitable to validate this approach [17].

TABLE I : Charge surface density (pc/m) on straight finite as a function of the resolutions levels

	Expansion Function			
Point	Haar Wavelet (Level)			Pulse
	2	3	4	
1	8.835	9.376	9.957	9.957
2	8.835	9.376	8.764	8.764
3	8.835	8.274	8.411	8.411
4	8.835	8.274	8.219	8.219

5	7.970	8.059	8.102	8.102
…	…	…	…	…
12	7.970	8.059	8.102	8.102
13	8.835	8.274	8.219	8.219
14	8.835	8.274	8.411	8.411
15	8.835	9.376	8.764	8.764
16	8.835	9.376	9.957	9.957

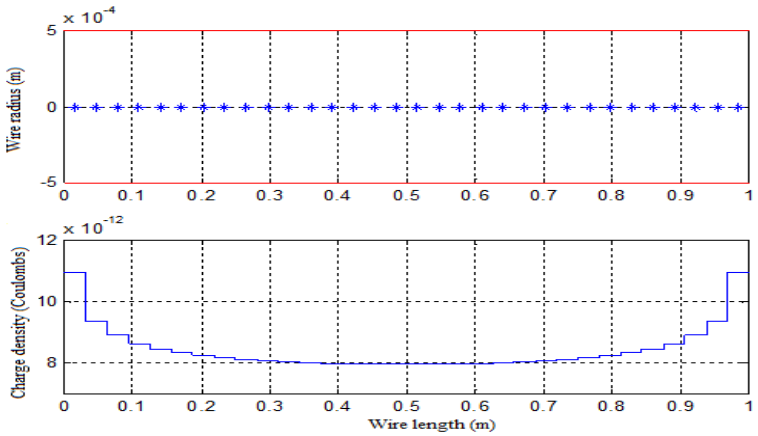

Fig. 7 - The surface charge (pC/m) on a 1.0m straight wire for 32 subdivisions

b. The thin plane plate

After applying the aforementioned formulation, some results were obtained. For example, the Fig. 8 represents the surface charge density in a square plate (1.0mx1.0m), submitted to a potential of 1.0 V. In this case, it was adopted 16 subdivision for each of the axes, and the level 5 of resolution was applied to the Wavelets. Concerning the characteristic of the method, it should be emphasized that the application of the Haar wavelets originates scattered matrixes. Thus, we will have nulls coefficients that can result in a computing time reduction.

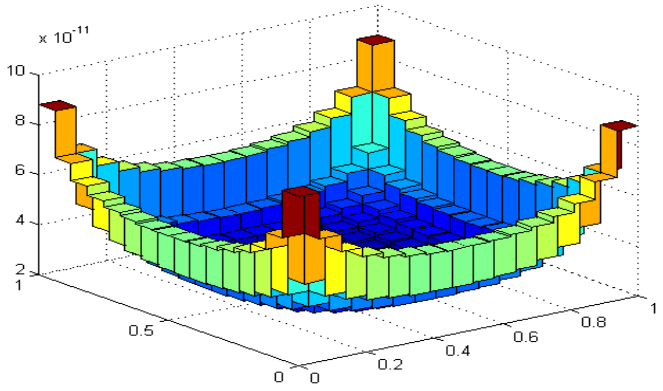

Fig. 8 - The surface charge (pC/m) on a 1.0 by 1.0m plate for 16 subdivisions

The Table II presents the comparative results, regarding the computing time values function of the adopted axe

division number, with or without applying the null value detection routine [18].

TABLE II : Computing time(s) function of the axe subdivisions and of the null value detection use

Divisions	Computing time (s)		Difference
Plane Plate	Without	With	(%)
4x4	0.321	0.25	22.12
8x8	7.931	5.488	30.80
16x16	451.960	222.60	50.75
32x32	27,273.738	11,994.487	56.02

In applying for a finite flat plate, we measured the execution time of the program, varying the number of divisions in each of the axes, measuring both the amount held in floating point operations as the runtime. The Table III shows the valuesobtained for the total execution time and the amount of floating point operations performed, using as expansion function the Haar wavelet.

TABLE III: Calculation floating point operations and the execution time depending on the number of divisions of the plate

Divisions	Floating point operations	Runtime (s)
4X4	29.075	0,321
8X8	1.236.699	7,931
16X16	70.025.893	451,96

Taking advantage of the fact that the Haar matrix is sparse, we reduce the execution time of the program by entering a comparison that, when the null value is detected, the transaction between the arrays is performed. The Table IV presents the results comparing the values of the runtime and the number of floating point operations, with and without detection of null values.

TABLE IV: Amount of floating point operations and execution time (s), depending on the number of divisions of the plate with and without detection of nulls

	Nulls value				Diference
Div.	Without detection		With detection		(%)
	Flops operation	Runtime	Flops operation	Runtime	Runtime
4X4	29.075	0,321	25.491	0,250	22,12
8X8	1.236.699	7,931	843.483	5,488	30,80
16X16	70.025.893	451,96	39.748.261	222,60	50,75

According to the results, reduced on average 40% run time of the program. The Fig. 9 (blue color) shows the values obtained for the runtime with and without detection of null values, depending on the number of divisions of finite flat plate.

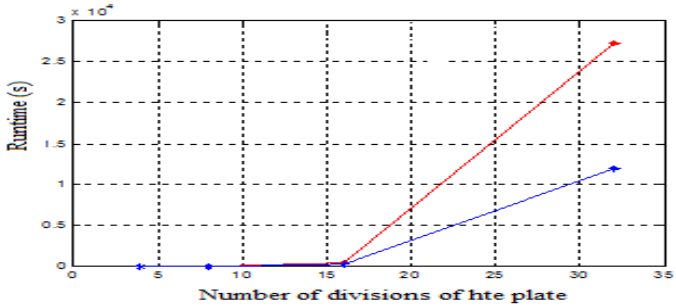

Fig.9 - The computing time (s) as a function of the subdivision axe number

When the plate was divided into 16 equal segments on each axis, a total of 256 coefficients were generated with

54% of them are zero. Taking advantage of the fact that the Haar matrix is sparse, applying the matrix algebra we can write that

$$[Z_{mn}] * [V] = [\quad] \qquad (34)$$

where, Z_{mn} is a square matrix that is not necessarily a scattered one, since it depends on the expansion function that was chosen. Thus, taking advantages of the fact that the Haar matrix is a scattered matrix, applying the matrix algebra, it will result [19]:

$$[Z'_{mn}] * [V'] = [\quad] \qquad (35)$$

else,

$$[Z'_{mn}] = [H]\,[Z_{mn}]\,[H^T] \qquad (36)$$

$$[\rho'] = [H^T]^{-1} * [\rho] \text{ and } [V'] = [H]\,[V] \qquad (37)$$

$$[H] \times [Z_{mn}] \times [H^T] \times [H^T]^{-1} \times [\quad] = [\quad] \times [\quad] \qquad (38)$$

As estimation, when the null value detection routine is carried using the null value detection routine. The Fig. 10 represents the Haar matrix and Fig. 11 and 12 presents the Z'_{mn} matrix configuration for the threshold equal to 0.01%, and 0.05%,
respectively. The dark part is the no null values.

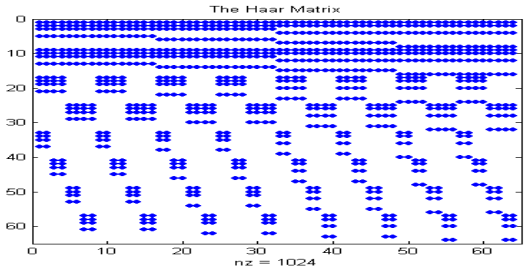

Fig.10 - The Haar matrix

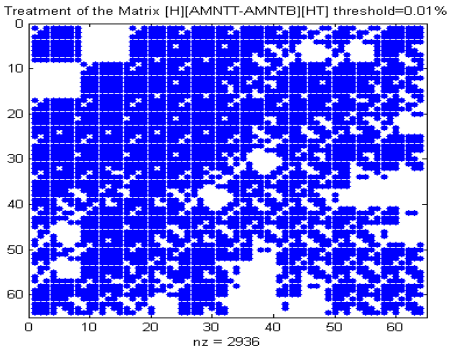

Fig.11 - Value of the threshold of 0.01% (23528 non-zero elements)

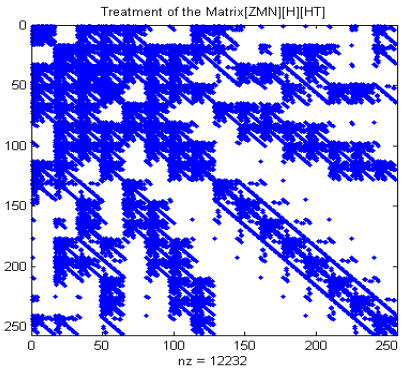

Fig. 12 - Value of a threshold of 0.05% (12232 non-zero elements)

The Table V, shows the computing time, when the threshold level and the axe subdivision number are taken into account.

TABLE V: Computing time(s) as a function of the axe subdivisions and of the adopted threshold level

Subdivision	Threshold levels (%)			
	0.00001	0.01	0.05	0.1
16x16	0.27	0.21	0.16	0.12
32x32	25.486	11.49	4.516	2.073

The Fig. 13 represents the error variation for the charge surface density, considering a square plane plate, and 16 axe subdivisions, as a function of the selected threshold.

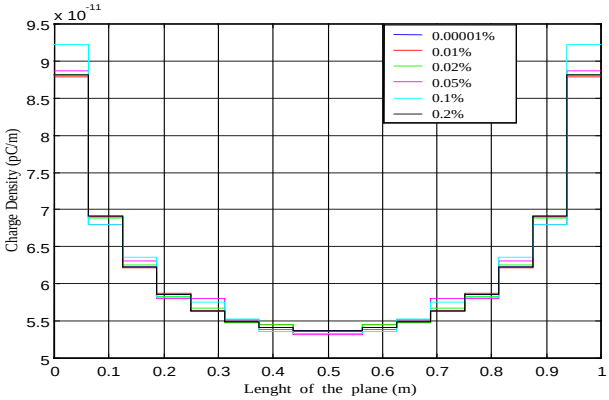

Fig. 13 - Variation of the charge surface density as a function of a selected threshold

Therefore, the variation of the threshold allowed a significant reduction in execution time without significantly changing the value of the surface charge density.Moreover, it should be mentioned that the Cholesky decomposition method were also implemented [8]. The Fig.14 represents the matrix configuration after applying it, assuming a threshold level equal to 0.01%. In this case, approximate increase of 64% was obtained in the null value element of the matrix.

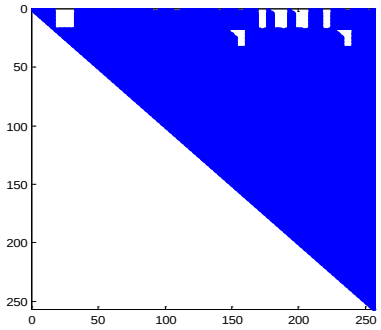

Fig. 14 - Matrix configuration after applying the Cholesky decomposition for the threshold equal to 0.01%

Regarding the computational performance, the average computing time decreased from 0.21 to 0.02 (s), for 16 axe subdivision, and a reduction time from 11.49 to 0.351(s).

c. Eddy current problem

In the application here presented, a copper conductor with the conductivity of 1.72 (μΩcm) and resistivity of 100% as shown on Table VI [20]. The Fig. 15 shows the reactions of the electromagnetic field and the involved energy considering the influence between the charges using the developed program.

TABLE VI: Material Characteristics

Material Type	Resistance (μΩcm)	Conductivity (%)
Aluminum (99.9)	2.65	64.84
Bronze	12	14
Copper	***1.72***	***100***
Nickel	37	4.5
Gold	2.36	76

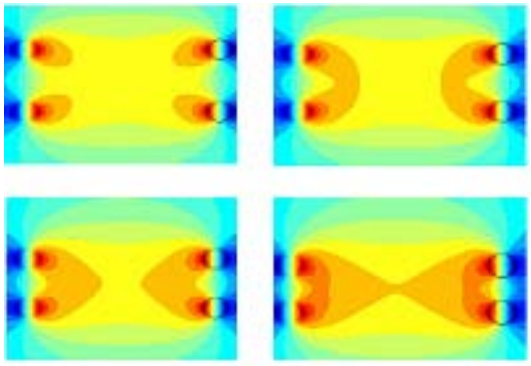

Fig. 15 - Electric field simulation

Therefore the final equation for each one of the elements that compose the current matrix can be expressed by:

$$A(x,y) = 1 - \frac{j\omega\mu\gamma}{4\pi} * h^2 *$$
$$*a_j b_j \int_{-a}^{a}\int_{-b}^{b} \ln\left[\phi(x,y)\left(\sqrt{(x_m - x_n)^2 + (y_m - y'_n)^2}\right)\right] dxdy +$$
$$+ \sum_{j=-\infty}^{\infty}\sum_{k=-\infty}^{\infty} a_{j,k} b_{j,k} * \qquad (39)$$
$$*\int_{-a}^{a}\int_{-b}^{b} \ln\left[x_{j,k}^{(H)}(\quad x)\left(\sqrt{(x_m + n y)^2 - (y_m \quad n)^2}\right)\right]$$

The solution of the previous equation can be obtained by using the expression $[a_{mn}]*[Coef]=[U_0]$ [21][22].
The Fig. 16 was obtained through the use of the application toolbox and shows the results of the coefficients in relation to the several resolution levels. The numerical values are available in the application as well [23]. It shows the statistical data for a 0.01% threshold with level 5 resolution.

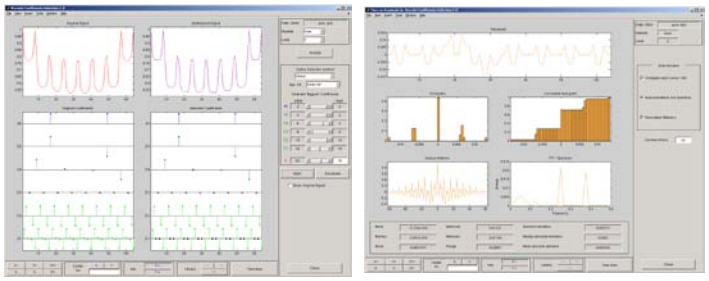

Fig. 16 - Wavelet Coefficients as a function of the resolution level and statistical data

IV. Conclusion

This article has simply a series of applications of wavelets, such as the surface density in a finite straight wire and a flat plate, and the determination of eddy currents using the pulse and as a expansion function of the Haar wavelet.
The proposed methodology permits the determination of the available numerical coefficients in the application as a function of the resolution level, this way avoiding the complex solution of the inner product, usually composed of double integrals that do not possess a very immediate solution.

By performing the product of the current matrix by the Haar wavelet $[a_{mn}][Coefficients][Haar]=[U_0][Haar]$ and in some cases reductions in execution time of up to 40% has been achieved.With this reduction in run time no significative variation in the a_{mn} elements that could compromise the final results has been found.Although the proposed application is relatively simple, the presented methodology is likely to be applied to problems of greater complexity, such as a refinement can be achieved in energy in locking electric motors, cardiac signals, transmission lines, electromagnetic compatibility, financial market, corrosion or thermal treatment, neurological treatments and etc.

REFERENCES

[1]*Field Computation by Moment Methods*, Harrington R. F., New York, Macmillan Company, 1968,2° ed. pp. 45-150.

[2] *A. Introduction to Electromagnetic Fields*, Clayton P. R. and Syed N.. New York, McGraw-Hill, 1998, 1°ed. pp.120-190.

[3]*Constantine A. B. Advanced Engineering Eletromagnetics*, York,John Wiley & Sons, 1989, 2°ed., 1989, pp. 670-695.

[4]*Harrington, R.F., Time-Harmonic Electromagnetic Fields*, Graw-Hill, New York, , 2°ed., 1998, pp. 220-312.

[5]Phillips, B.L. A technique for the numerical solution of certain integral equations of the second kind, 1962.

[6]Liang J.; Elangovan S.; Devotta J. B. X. A Wavelet Multiresolution Analysis Approach to Fault Detection and Classification in Transmission Lines. Elsevier Computer physics communications, 1999, pp.327-332.

[7]Mallat S. Wavelets for a Vision. IEEE Proceedings of the IEEE, vol 84, N°4, 1996, pp.604-614.

[8]Cohen A. ; Kovacevic J. Wavelets: The mathematical background. IEEE Proceedings of the IEEE, vol 84, N°4, 1996 pp.514-522.

[9] *Ondas e Ondaletas*, Morettin P. A., 1°ed, São Paulo, Edusp, 1999, pp. 1-55.

[10] *7°Escola de Séries Temporais e Econometria*, Morettin P. A. 1° ed, São Paulo, Edusp, 1997, pp. 20-34.

[11] *Random Vibrations Spectral and Wavelet Analysis*, D. E. Newland, , Addison Wesley Longman, 1° ed, 1993, pp. 315-333.

[12] *Discovering Wavelets*, Aboufadel E.; Schlicker S. John Wiley & Sons 1999, pp. 1-42.

[13] Kriezis E.E.; Stavaros M. P.,Tegopoulos J. A., "Eddy Currents: Theory and Applications", Proceedings of the IEEE, vol. 80, N° 10, 1992.

[14] Lopez L. A N. M., Transformadas de Wavelet e Lógica Fuzzy na Inspeção por Eddy-Current em Tubos de Geradores de Vapor de Centrais Nucleares, Tese de Doutorado,Universidade de São Paulo, USP, Brasil, 2003.

[15]Stoll, R. L., The analysis of eddy currents, Clarendon Press, 1974.

[16] Kaitec, "The 14th Kori Unit 4 Steam Generator Tube Eddy Current Examination – Final Report", Nov. 2004.

[17]Belardi A. A. ,Cardoso J. R., Sartori C. F.,Wavelets "Application in Electrostatic and their Computing Aspects", Germany Aachen EMF 2003, 2003, pp. 43-46.

[18]Belardi A. A. ,Cardoso J. R., Sartori C. F., "Application of Haar's Wavelets in the method to solve electrostatic problems", Compel Vol. 23, N°3, 2004, pp. 606-612.

[19] *Numerical Linear Algebra and Applications*, Datta B. N, 1.ed. New York, Brooks/Cole Publishing Company 1995, pp. 222-225

[20]KPS, The 5th Ulchin Unit 4 Steam Generator Tube Eddy Current Examination – Final Report", Mar. 2005.

[21]Bossavit, A. , A numerical approach to transient nonlinear eddy current problems in applied electromagnetic in materials, Elsevier, 1990.

[22] Salon S., Peng J.P.,Three dimensional eddy currents using a four component finite element formulation IEEE Transactions on Magnetics, 1994.

[23]Palm, W., Introduction to Matlab and Simulink for Engineers, McGraw-Hill,2010, pp. 55-97.

Authors Biography

Aldo Artur Belardi was born in 1953. He graduated in Electrical Engineering in 1978 on Faculdade de Engenharia Industrial FEI, Brazil. Ph.D on Escola Politécnica da Universidade de São Paulo (EPUSP), Brazil in 2003. His doctoral research was: "Contribution of Wavelets Application in Electrostatic". His teaching and research areas of interest include numerical techniques and application in electrostatic, electromagnetic and scattering and neuroscience.

Antonio H. Neto Piccinini was born in 1991.He graduated in Electrical Engineering, in 2012 on Centro Universitário da FEI and is a Master student from Centro Universitário da FEI, Brazil. His research areas of interest include sustainable energy, numerical techniques, and Wavelets Applications.